



## A model for an electronic spiking neuron built with a memristive voltage-gated element

Leandro E. Fernandez<sup>a,b</sup>, Agustin Carpio<sup>a,b</sup>, Jiaming Wu<sup>d</sup>, Stefano Boccaletti<sup>c,e</sup>,  
Marcelo Rozenberg<sup>d</sup>, Gabriel B. Mindlin<sup>a,b,e,\*</sup>

<sup>a</sup> Departamento de Física, Facultad de Ciencias Exactas y Naturales, Universidad de Buenos Aires, Argentina

<sup>b</sup> INFINA, CONICET, Argentina

<sup>c</sup> Institute for Complex Systems, CNR, Florence, Italy

<sup>d</sup> LPS, CNRS, Orsay, France

<sup>e</sup> Departamento de Matemática aplicada, Universidad Rey Juan Carlos, Mostoles, Spain

### ARTICLE INFO

#### Keywords:

Electronic neurons  
Dynamics  
Bifurcations

### ABSTRACT

This study introduces a mathematical model for an electronic circuit capable of emulating both spiking and bursting neurons. The circuit incorporates a memristor as the nonlinear element essential for generating excitable dynamics. Our demonstrations illustrate that the model's solutions effectively capture the qualitative features of circuit voltages and currents. Additionally, we provide interpretations of these qualitative characteristics in the context of the underlying dynamics of the system.

### 1. Introduction

Nerve cells within the nervous system, as well as muscle cells, are collectively referred to as excitable tissues, exhibiting intricate electrical behaviors. Indeed, their behaviors have been elucidated in terms of fundamental electric phenomena, and the equations that characterize them have formed the foundation for mathematical models utilized in theoretical neuroscience [1,2]. A notable endeavor has been the physical realization of electronic equivalent circuits that simulate excitable tissues—these devices are known as electronic neurons. The physical embodiment of these electronic circuits serves two primary objectives. Firstly, it enables the validation of the representational accuracy of models for excitable tissues, ensuring that the circuits emulate the behaviors of the tissues they intend to model. Secondly, it seeks to engineer circuits endowed with specific behaviors, facilitating information processing in a manner analogous to natural processes [3]. This is particularly valuable for practical applications. A growing interest in these devices lies in the therapeutic potential of targeted modulation of electrical activity in the peripheral nervous system, entailing two technical challenges: the development of interfaces that enable long-term nerve control and monitoring, as well as the creation of compact, responsive devices capable of generating real-time stimuli. Electronic neurons are an innovative solution to address this latter challenge.

Electronic neurons boast a substantial and diverse history. Certain circuits are designed to implement analog integrations of phenomenological models that describe the behavior of neuron membranes. These models commonly embody the membrane's excitatory mechanisms, serving as electronic realizations of Hodgkin and Huxley's theoretical membrane model [3]. Others concentrate on replicating the dynamic attributes of excitability. This is achieved through either the construction of analog integrators for dynamic equations that exhibit excitability [4], or by employing nonlinear devices that exhibit excitable dynamics [5].

Significant efforts are also dedicated to implement electronic neurons in CMOS (Complementary metal-oxide-semiconductor) VLSI (very large-scale integration) technology [6], as miniaturization allows the fabrication of massive numbers of neurons [7,8]. However, this is done at the expense of flexibility, since the chip design may take several years. Moreover, miniaturization usually leads to spiking frequencies that are several orders of magnitude above that of biological neurons, which render the interfacing difficult. We may also mention, in this non-exhaustive introduction, the neuromorphic processors, such as Intel's Loihi [9] and IBM's TrueNorth [10], which essentially optimize digital computer architectures to simulate neural network systems. Finally, another promising approach is to employ programmable Field-Programmable Gate Arrays (FPGAs), capitalizing on the computational

\* Corresponding author at: Departamento de Física, Facultad de Ciencias Exactas y Naturales, Universidad de Buenos Aires, Argentina.

E-mail address: [gabo@df.uba.ar](mailto:gabo@df.uba.ar) (G.B. Mindlin).

<https://doi.org/10.1016/j.chaos.2024.114555>

Received 10 December 2023; Accepted 30 January 2024

Available online 10 February 2024

0960-0779/© 2024 Elsevier Ltd. All rights reserved.

prohess of these specialized processors [11,12]. Many of these endeavors have centered on simulating expansive arrays of excitable units.

Here, we follow a very different approach that focus on the implementation of arguably the simplest electronic circuit realization of an excitable system. Recently, a novel spiking neuron model has been introduced, in which the memristor serves as the nonlinear element responsible for obtaining excitable dynamics [13]. A memristor, in simple terms, is a two-terminal resistive component that exhibits variable resistance, which depends on the past applied voltage (or current), hence, that exhibits a hysteresis, or memory, effect. We employ a novel volatile memristor trivially formed by combining two conventional electronic components: a resistor (R) and a thyristor (T). The resistor is simply connected to the anode and to the gate of the thyristor. The two-terminal memristor device is obtained between the anode and the cathode [14]. The memristor has the function of a voltage-controlled switch, hence, by connecting a capacitor (C) in parallel one obtains a *leaky-integrate-and fire* neuron model. Indeed, each function is implemented by each component: the C *integrates*, the R *leaks* and, critically, the T *fires*. Remarkably, this electronic neuron hence achieves the simplest possible implementation of the LIF neuron model. This basic circuit can be used as stepping stone to implement large variety of biologically relevant spiking behaviors [15]. A conceptually important point to realize is that our neuron model is actually defined through its hardware implementation—an electronic circuit. As we shall show here, its nonlinearities share the same nature with standard mathematical neuron models. Significantly, this paves a novel way for constructing intricate arrays of devices that should provide novel insights on the collective behavior of neural networks, i.e. to build neural network simulators of unprecedented simplicity and ultra-low cost.

In this study, we present a mathematical model for the circuit and demonstrate that its solutions can capture the qualitative aspects of circuit voltages and currents. Furthermore, we interpret these qualitative characteristics in terms of the underlying dynamics of the problem.

## 2. The model

### 1. The electronic neuron

The Memristive Spiking Neuron model we will be examining is an electronic neuron comprised of two distinct blocks. The first one is composed of a capacitor connected to a memristor, which realize the basic LIF model of a regular (i.e. tonic) spiking neuron that we described above [13]. The second block simply consists of a capacitor in parallel with a resistance and extends the LIF model to generate bursts of spikes [14]. If we ignore for the moment the second block, we may understand the simple mechanism of spike generation of the first block. Injecting current into the shared terminal of the capacitor and the memristor, which is initially in its “open” (i.e. high resistance) state, causes the former to charge. When the potential in the capacitor reaches a threshold value of  $V_{th}$ , there is a dramatic decrease of the resistance of the memristor, as in the closure of an electric switch, which results in a current spike due to the sudden discharge of the capacitor.

The role of the second block is to introduce an additional temporal scale in the model:  $\tau_s = R_s C_s$ .

Our two-block electronic neuron, termed Memristive Spiking Bursting Neuron (MSBN) model, can be interpreted as a two-compartment model, with one compartment representing the dendrite and the other representing the soma (Fig. 1). It is somewhat inspired by a well-known biological bursting neuron model introduced by Pinsky and Rinzel [16], that consists of two compartments coupled by a conductance denoted as  $g_c$ . In the MSBN model, the two compartments are directly connected, akin to the limit of strong electrotonic coupling (large  $g_c$ ) in the Pinsky and Rinzel model.

Remarkably, this seemingly uncomplicated circuit manifests intricate dynamic behavior, characterized by four distinct regions displaying varying spiking patterns and two restful zones. These patterns arise from

the interplay of the input current ( $I_{in}$ ) and the time constant ( $\tau_s$ ) of the soma compartment. When the value of  $\tau_s$  is low, a phenomenon known as Tonic Spiking (TS) occurs. Through the control of the parameters of  $\tau_s$  and  $I_{in}$ , we can elicit tonic spikes with differing intensities, durations, and intervals, as illustrated by the three red plots on the right side of the figure. This phenomenon is expected due to the relatively short time constant in the soma, compared to the dendritic components. In other words, the capacitor  $C_s$  is small, hence charging very fast, resulting in a negligible perturbation to the emergence of the Tonic Spiking behavior that we described before.

As the value of  $\tau_s$  is gradually increased, it becomes relevant with respect to the discharge time-scale ( $\tau_{spike}$ ), hence can no longer be perceived as a minor perturbation. This leads to the manifestation of Fast Spiking (FS) behavior, distinct from the TS, and found in the large blue region that dominates the phase diagram of Fig. 1 at large  $\tau_s$ . It is interesting to note that this novel spiking behavior also brings about two additional forms of dynamical behavior, which are intrinsic bursting and designated as IB1 and IB2 (green and yellow regions in the phase diagram). We may note that these two types of bursting emerge correspondingly at the onsets of excitability of the Fast Spiking state for both, low and high input current ( $I_{in}$ ). It is noteworthy that IB1 exhibits bursts that, during non-firing periods, exhibit prolonged proximity to the lower fixed point. Conversely, IB2 displays a similar pattern around the upper fixed point.

Similarly, the identical principle applies to the Fast Spiking behavior, wherein altering parameters shifts the reference point for oscillations. This change is evident in the blue panels on the right. Analogously, distinct burst durations and intervals emerge for IB1 and IB2 due to variations in parameters. This is visually represented in the right panel, where yellow and green depict the characteristics of IB1 and IB2.

Despite the circuit’s simplicity it has a remarkably rich emergent dynamical behavior. This is due to a variety of non-linearities in competition and their ensuing bifurcations. The goal of the present work is to introduce a mathematical description of the circuit that allows for the systematic exploration and understanding of those dynamical instabilities. This study is a necessary starting point to envision the exploration and rationalization of the even richer collective behavior that may emerge from networks of coupled MSBNs.

### 2. Equations of the MSBN model

Constructing a comprehensive set of equations for this model entails two essential components. The first component involves a set of Kirchhoff equations, which account for both charge conservation and the requirement of zero net voltages along closed paths within the circuit. The second component necessitates a dynamical model that describes the transition of the circuits to either of the two resistive modes of the memristor.

To effectively capture this dynamic process, we propose a simple method of rapid convergence toward either a state of high or low resistance. To describe a system with memory, we need a dynamical system capable of exhibiting diverse behaviors based on distinct initial conditions within a range of voltages. This intricate behavior can be encapsulated by a vector field resulting from the computation of the universal unfolding of a Pitchfork bifurcation [17]:

$$\dot{I}_m = I_m^*(V_m - a) + b^*I_m^2 - c^*I_m^3 + d \quad (1)$$

In this unfolding, two terms, parametrized by  $d, b$ , introduce asymmetry that breaks the reflection symmetry. As long as  $d < b^3/27$ , the system exhibits bistability. For small voltages, regardless of the initial current, the system converges to a regime of high resistance (resulting in an attracting state characterized by an extremely low current). Conversely, under large voltages, the resistance experiences a substantial reduction (leading to dynamics that result in an attractor with high current values). Notably, a captivating phenomenon occurs within an

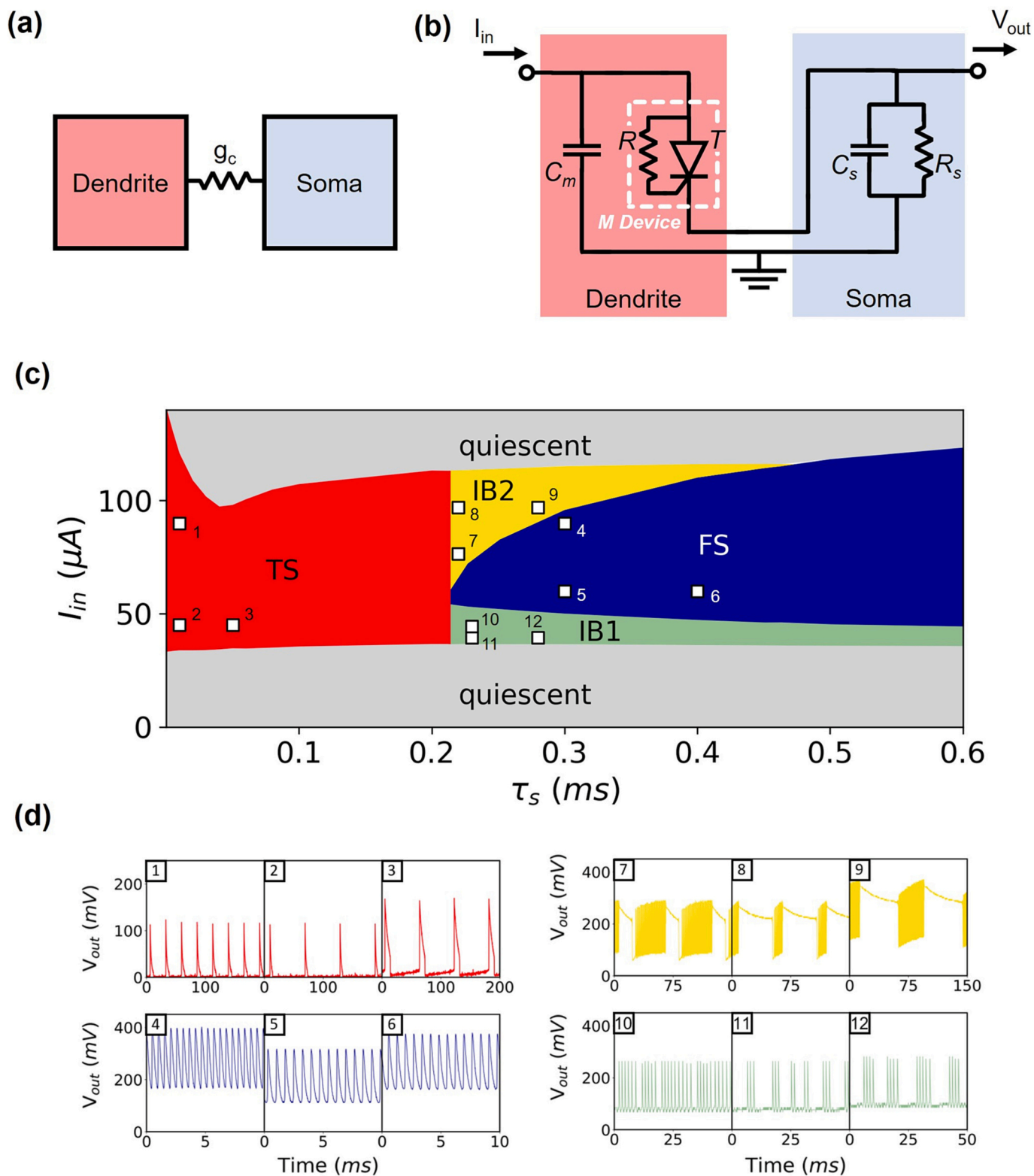


**Fig. 1.** The experimental measurements of the electronic neuron. The device naturally reproduces a set of behaviors that cover the spectrum of dynamical processes found in nature. In a), we display a basic two compartments model for a neuron, whose dynamics can be reproduced by the device shown in b), where the nonlinear device is a thyristor. In c) we show different regions of the parameter space where different behavior was reported. Typical time series found in each of the regions are displayed in d). The color used in the time traces matches the color of the region. The figure is adapted from [14], and therefore the criterium used to classify the solutions is the one described in that reference. Basically, the color gray indicates quiescent states (i.e. fixed points), blue for fast periodic solutions, periodic sequences of spikes are indicated with red, and blue and green are used for bursting solutions. The difference between those solutions refers to how much time the bursting solutions spend close to the on or the off state. (For interpretation of the references to color in this figure legend, the reader is referred to the web version of this article.)

interval of voltages across the memristor—within this interval, the system converges to either a high or low resistance regime based on the initial condition. This phenomenon contributes to the device’s characteristic memory. The selection of problem parameters ensures that the convergence to either regime transpires significantly faster than any other dynamical process within the problem.

The principle of current conservation at the junction of the branches holding  $R_s$  and  $C_s$  gives rise to the following equation:

$$V'_{out} = \frac{1}{C_s} * \left( I_m - \frac{V_{out}}{R_s} \right) \quad (2)$$

while the zero-sum rule for the voltages allow us to relate the voltage across the memristor to the other variables of the problem:

$$V'_m = \frac{I_{in}}{C_m} - I_m * \left( \frac{1}{C_m} + \frac{1}{C_s} \right) + \frac{V_{out}}{R_s C_s} \quad (3)$$

The Eqs. (1)–(3) constitute a dynamical system capable of displaying rich and diverse solutions. In the following section we describe some of interesting dynamics interpretable in terms of neural spiking and bursting behavior.

### 3. Results

The Eqs. (1)–(3) describe the dynamics of our model. Being a 3d dynamical system, it can display a variety of attractors, from fixed point, periodic solutions, quasiperiodic behavior and even chaos. Given a set of parameters  $(a, b, c, d, C_s, C_m, \tau_s, I_{in})$ , we can numerically integrate the temporal evolution of the state of the system  $(V_{out}, V_m, I_m)$  by specifying the initial conditions  $(V_{out}(0), V_m(0), I_m(0))$ . Due to the system’s hysteresis nature, qualitatively different solutions emerge for different initial conditions in certain parameter space regions. We examined the solutions across a grid of  $\tau_s$  and  $I_{in}$  values, with a focus on two pivotal aspects. The first aspect—topological in nature—pertains to the periodicity of the solution. This periodicity is evaluated by counting the number of crossings with a Poincaré section ( $V_{out} = 0$ , taking the positive-oriented flow direction crosses). To facilitate a comparison of

our dynamical system’s analysis results with previous findings on the electronic neuron, we introduced a bursting coefficient. This coefficient, indicative of the proportion of time during which the solution remains above the median amplitude, enables meaningful comparison.

The numerical simulations used to generate Fig. 2 were carried out with  $(a, b, c, d, C_s, C_m) = (10, 4.85, 0.594, 0.1, 0.1, 10)$  and parameters  $\tau_s$  and  $I_{in}$  sampled from a  $1200 \times 600$  grid with  $\tau_s \in (0.01, 0.35)$  and  $I_{in} \in (0.01, 3.0)$ . The grid displayed in the figure was integrated “upward”, that is, each numerical simulation was initialized with initial conditions  $(V_{out}(0), V_m(0), I_m(0))$  equal to  $(V_{out}(T), V_m(T), I_m(T))$ , taken from the prior run for the same  $\tau_s$  and the immediately lower  $I_{in}$  (except for the bottom row of the grid, where integration commenced in proximity to the stable fixed point associated with the Quiescent State), being  $T$  the total integration time.

Upon examination of Fig. 2, we discern the identification of two distinct and well-defined regions that correspond to 1-periodic solutions. The blue region mirrors the experimental Fast Spiking behavior showcased in Fig. 1. Conversely, the red region illustrates slower solutions characterized by extended periods, akin to the Tonic Spiking behavior. In addition, we extend this analysis to include 2, 3 and 4-periodic solutions whose growth rates differ significantly from the decrement rates. Specifically, we consider those solutions for which the time spent in the growth phase is equal to or less than 10 % of  $T$ .

Moreover, a correspondence emerges between the computationally derived bursting solutions and the depicted IB1 and IB2 behaviors in Fig. 1. Solutions corresponding to a low bursting coefficient (indicated by greener shades) align with patterns wherein bursts of brief spikes alternate with periods of low activity, akin to ‘silences.’ In contrast, solutions corresponding to a high bursting coefficient (indicated by yellower shades) are better described by prolonged periods of high amplitude, with spikes occurring before transitioning back to the low amplitude phase.

By studying the equations that describe the dynamics of the device, we gain insight into the type of behavior that can be anticipated when large arrays of these units are interconnected. Communication between these units can be categorized into electrical and chemical synapses. These two types of synapses fundamentally differ in their transmission

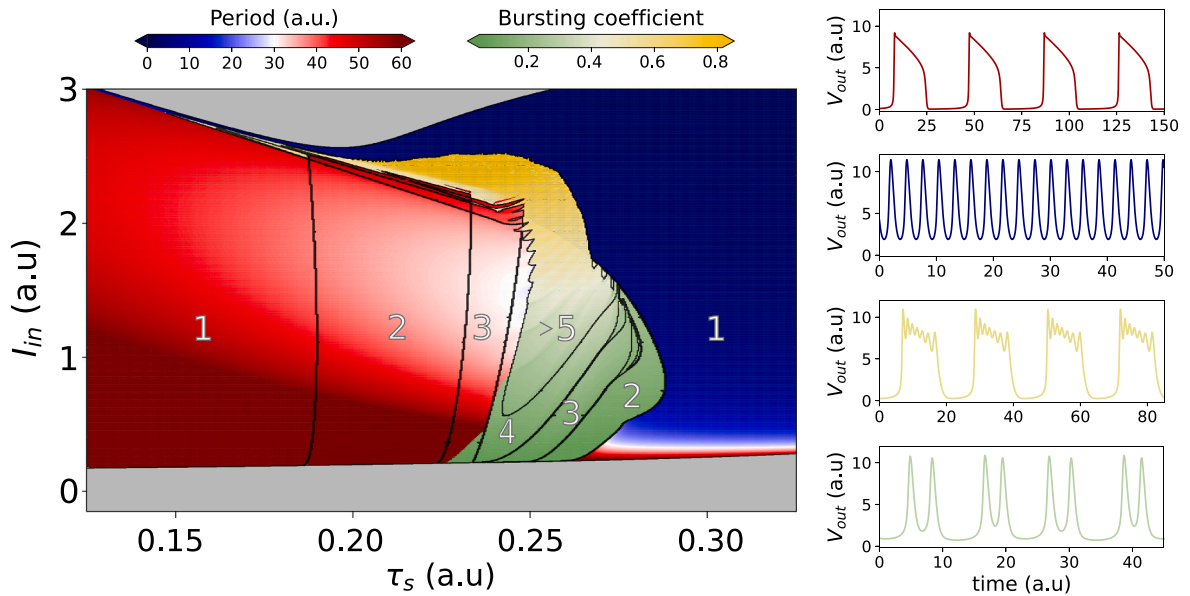


Fig. 2. The numerical simulations used to generate Fig. 2a were carried out with  $(a, b, c, d, C_s, C_m) = (10, 4.85, 0.594, 0.1, 0.1, 10)$ ,  $\tau_s \in (0.01, 0.35)$  and  $I_{in} \in (0.01, 3.0)$ , within a grid of  $1200 \times 600$ . The left panel separates the parameter space in regions according to the  $n$ -periodicity of the solutions, it also employs a distinctive color scheme: gray represents the Quiescent state, a gradient spanning from blue to red signifies the period of 1-periodic solutions and the 2, 3 and 4-periodic solutions whose derivative spends less than 10 % in the positive range, and a gradient from green to yellow indicates the bursting coefficient for the other cases. The right panels are representative plots of  $V_{out}$  for different zones of the grid. The color is equivalent to the one in the left panel from which the values of  $\tau_s$  and  $I_{in}$  were sampled. (For interpretation of the references to color in this figure legend, the reader is referred to the web version of this article.)

mechanisms. In electrical synapses, intercellular channels known as gap junctions exist between pre- and postsynaptic membranes, allowing current to flow passively. This flow of ionic current occurs through the gap junction pores, enabling current to move from one neuron to another. The typical source of this current is the local potential difference generated by the action potential. For these specific diffusive couplings, the model that describes the dynamics belongs to what is known to be the class II, according to the Master Stability Function approach [18,19]. Class II systems are of particular importance, as they can be used as units of a network able to perform parallel computation. Indeed, from one side it is guaranteed that, given whatever connection structure in the network, complete synchronization will be always stable for coupling strengths larger than a given threshold. From the other side, given any specific (desired) cluster of units it is guaranteed that a network structure exists where the units of such cluster are capable of synchronizing, also independently on the dynamics of any other units not belonging to the cluster. This latter property implies that one can always architecture a topology of connection for which desired parallel clusters synchronize at will [20].

In contrast, when dealing with chemical synapses, the challenge of unraveling the global dynamics of a large set of coupled excitable units remains open. Notable progress has been made in understanding how collective dynamics emerge as phase oscillators are coupled, even for non-diffusive coupling [21]. However, for three-dimensional systems that exhibit complex dynamics at the level of elementary units, the problem remains an ongoing challenge.

#### 4. Conclusions

In recent times, an electronic device has been introduced that showcases dynamic regimes in which the time series of one of its variables resembles a diverse array of biologically significant features, akin to those exhibited by neurons in the nervous system. These regimes encompass periodic spiking, bursting, and excitable quiescent states. Throughout history, there exists a wealth of electronic devices capable of analogically integrating equations that describe the electric properties of nervous system tissues. However, in this instance, a simple nonlinear memristive device coupled with a few passive elements serves as the cornerstone for generating a wide spectrum of behaviors. In the course of this work, we formulated the equations that define such a unit and successfully demonstrated that their solutions aptly capture the dynamical characteristics of the electronic neuron.

By simplifying the circuit to its minimum complexity and identifying the fundamental dynamical elements required to replicate the solutions, we embark on an intriguing avenue to potentially scale the production of electronic neurons. In this context, we recognize the relevant role of the concept of memristance, which provides the switch-like functionality that is at the root of the LIF neuron model. Our present approach is based on discrete, conventional electronic components, however our this can be considered as the initial steps of an ambitious novel road map for the future hardware fort artificial intelligence. In fact, quite remarkably, the memristor device at the heart of the present neuron model can be realized by a type of quantum materials showing a fascinating insulator to metal transition, which are known as Mott insulators. Those materials are receiving a great deal of attention for their potential neuromorphic functionalities [22], as their theoretical understanding and reliable fabrication remains an open challenge [23–25]. Overcoming those challenges and understanding the dynamical behavior of neuron models based on memristors will paved the way for the implementation of novel hardware for artificial intelligence in the 21st century and beyond.

#### CRedit authorship contribution statement

**Leandro E. Fernandez:** Data curation, Formal analysis,

Visualization. **Agustin Carpio:** Data curation, Investigation, Visualization. **Jiaming Wu:** Data curation, Formal analysis, Software. **Stefano Boccaletti:** Conceptualization, Writing – original draft, Writing – review & editing. **Marcelo Rozenberg:** Conceptualization, Writing – original draft, Writing – review & editing. **Gabriel B. Mindlin:** Conceptualization, Formal analysis, Funding acquisition, Investigation, Methodology, Software, Supervision, Validation, Writing – original draft.

#### Declaration of competing interest

We declare no conflicts of interest, and that this manuscript has not been submitted to other journals.

#### Data availability

Data will be made available on request.

#### Acknowledgements

This grant was partially funded by ANCYT, PICT 2021 00965.

#### References

- [1] Koch C. *Biophysics of computation: information processing in single neurons*. Oxford University Press; 2004.
- [2] Izhikevich EM. *Dynamical systems in neuroscience*. MIT Press; 2007.
- [3] Malmivuo J, Plonsey R. *Bioelectromagnetism: principles and applications of bioelectric and biomagnetic fields*. Oxford University Press; 1995.
- [4] Aliaga J, Busca N, Mincas V, Mindlin GB, Pando B, Salles A, et al. Electronic neuron within a ganglion of a leech (*Hirudo Medicinalis*). *Phys Rev E* 2003;67:061915.
- [5] Medeiros BNS, Mincas V, Mindlin GB, Copelli M, Leite JRR. An excitable electronic circuit as a sensory neuron model. *Int J Bifurcat Chaos* 2012;22:1250244.
- [6] Weste NHE, Harris DM. *CMOS VLSI design: a circuits and systems perspective*. Pearson Education India; 2015.
- [7] Indiveri G, et al. Neuromorphic silicon neuron circuits. *Front Neurosci* 2011;5.
- [8] Thakur CS, et al. Large-scale neuromorphic spiking array processors: a quest to mimic the brain. *Front Neurosci* 2018;12.
- [9] Davies M, et al. Loihi: a neuromorphic manycore processor with on-chip learning. *IEEE Micro* 2018;38:82.
- [10] Merolla PA, et al. A million spiking-neuron integrated circuit with a scalable communication network and interface. *Science* 2014;345:668.
- [11] Pani D, Meloni P, Tuveri G, Palumbo F, Massobrio P, Raffo L. An FPGA platform for real-time simulation of spiking neuronal networks. *Front Neurosci* 2017;11.
- [12] Joucla S, Ambroise M, Levi T, Lafon T, Chauvet P, Saighi S, et al. Generation of locomotor-like activity in the isolated rat spinal cord using intraspinal electrical microstimulation driven by a digital neuromorphic CPG. *Front Neurosci* 2016;10.
- [13] Rozenberg MJ, Schneegans O, Stoliar P. An ultra-compact leaky-integrate-and-fire model for building spiking neural networks. *Sci Rep* 2019;9:1.
- [14] Wu J, Wang K, Schneegans O, Stoliar P, Rozenberg MJ. Bursting dynamics in a spiking neuron with a memristive voltage-gated channel. To appear in *neuromorphic computing and engineering*. 2023.
- [15] Stoliar P, Schneegans O, Rozenberg MJ. Biologically relevant dynamical behaviors realized in an ultra-compact neuron model. *Front Neurosci* 2020;14.
- [16] Pinsky PF, Rinzel J. Intrinsic and network rhythmogenesis in a reduced Traub model for CA3 neurons. *J Comput Neurosci* 1994;1:39.
- [17] Golubitsky M, Stewart I, Schaeffer DG. *Singularities and groups in bifurcation theory* Volume II. Springer Science & Business Media; 2012.
- [18] Pecora LM, Carroll TL. Master stability functions for synchronized coupled systems. *Phys Rev Lett* 1998;80:2109.
- [19] Boccaletti S, Latora V, Moreno Y, Chavez M, Hwang D-U. *Complex networks: structure and dynamics*. *Phys Rep* 2006;424:175.
- [20] Bayani A, Nazarimehr F, Jafari S, Kovalenko K, Contreras-Aso G, Alfaro-Bittner K, et al. The transition to synchronization of networked systems. <https://arxiv.org/abs/2303.08668v1>.
- [21] Ott E, Antonsen TM. Low dimensional behavior of large systems of globally coupled oscillators. *Chaos Interdiscip J Nonlinear Sci* 2008;18:037113.
- [22] Hoffmann A, et al. Quantum materials for energy-efficient neuromorphic computing: opportunities and challenges. *APL Mater* 2022;10:070904.
- [23] del Valle J, et al. Subthreshold firing in Mott nanodevices. *Nature* 2019;569:7756.
- [24] del Valle J, et al. Spatiotemporal characterization of the field-induced insulator-to-metal transition. *Science* 2021;373:907.
- [25] Adda C, et al. Direct observation of the electrically triggered insulator-metal transition in  $V_3O_5$  far below the transition temperature. *Phys Rev X* 2022;12:011025.